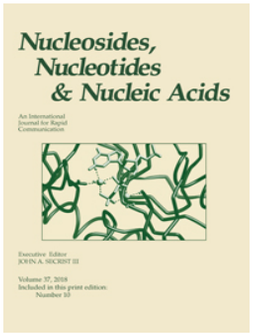

Nucleosides, Nucleotides and Nucleic Acids

ISSN: 1525-7770 (Print) 1532-2335 (Online) Journal homepage: https://www.tandfonline.com/loi/lncn20

DNA binding, photocleavage, antimicrobial and cytotoxic properties of Ru(II) polypyridyl complexes containing BOPIP ligand, (BOPIP = {2-(4-(benzyloxy) phenyl)-1H-imidazo [4,5-f] [1,2]phenanthroline})

Srinivas Gopu, Vuradi Ravi kumar, Kotha Laxma Reddy, Putta Venkat Reddy & Satyanarayana Sirasani

To cite this article: Srinivas Gopu, Vuradi Ravi kumar, Kotha Laxma Reddy, Putta Venkat Reddy & Satyanarayana Sirasani (2019): DNA binding, photocleavage, antimicrobial and cytotoxic properties of Ru(II) polypyridyl complexes containing BOPIP ligand, (BOPIP={2-(4-(benzyloxy) phenyl)-1H-imidazo [4,5-f] [1,2]phenanthroline}), Nucleosides, Nucleotides and Nucleic Acids, DOI: 10.1080/15257770.2018.1549329

To link to this article: https://doi.org/10.1080/15257770.2018.1549329

Published online: 19 Mar 2019.

NUCLEOSIDES, NUCLEOTIDES AND NUCLEIC ACIDS
https://doi.org/10.1080/15257770.2018.1549329

DNA binding, photocleavage, antimicrobial and cytotoxic properties of Ru(II) polypyridyl complexes containing BOPIP ligand, (BOPIP = {2-(4-(benzyloxy) phenyl)-1H-imidazo [4,5-f] [1,2]phenanthroline})

Srinivas Gopu[a,b], Vuradi Ravi kumar[a], Kotha Laxma Reddy[a], Putta Venkat Reddy[a], and Satyanarayana Sirasani[a]

[a]Department of Chemistry, University College of Science, Osmania University, Hyderabad, Telangana State, India; [b]Department of Chemistry, Government Degree College Manthani, Peddapalli District, Telangana State, India

ABSTRACT

A novel ligand BOPIP (BOPIP = {2-(4-(benzyloxy)phenyl)-1H-imidazo[4,5-f][1,10]phenanthroline}) and its mononuclear Ru(II) polypyridyl complexes $[Ru(phen)_2\ BOPIP]^{2+}$**(1)** (phen = 1,10-Phenanthrolene), $[Ru(bpy)_2\ BOPIP]^{2+}$**(2)** (bpy = 2,2′ bipyridyl), $[Ru(dmb)_2\ BOPIP]^{2+}$**(3)** (dmb = 4, 4′ -dimethyl 2, 2′ -bipyridine), $[Ru(Hdpa)_2\ BOPIP]^{2+}$**(4)** (Hdpa = 2,2′dipyridylamine) have been synthesized successfully and characterized by elemental analysis, UV-vis, IR, ^{1}H, ^{13}C-NMR, and ESI-MS Spectroscopy. The interaction of these complexes with CT-DNA was studied using absorption, emission techniques, viscosity measurements and molecular docking studies. The docking study also supports the binding ability of complexes obtained through the absorption and emission techniques. These studies reveal that the Four Ru(II) polypyridyl complexes bind to DNA predominantly by intercalation. The Antimicrobial activity and cytotoxicity of these complexes are also reported.

ARTICLE HISTORY
Received 13 August 2018
Accepted 9 November 2018

KEYWORDS
Antimicrobial activity; DNA binding; MTT Assay; Molecular Docking; Photocleavage; Viscosity

1. Introduction

Cancer is mostly considered as a group of dreadful diseases, characterized by uncontrolled cell growth. Cancer, still proven to be one of the unruliest diseases to which humans are subjected, and as yet no practical and completely effective drugs or methods to control are available. Hence, identification of new effective, selective, and less cytotoxic anticancer agents is still one of the most pressing health issues.[1–4] DNA, the carrier of genetic information, has been identified as the primary target for a variety of anticancer drugs because of their ability to interfere DNA transcription

CONTACT Satyanarayana Sirasani ssnsirasani@gmail.com Department of Chemistry, University College of Science, Osmania University, Hyderabad 500007, Telangana State, India.
Color versions of one or more of the figures in the article can be found online at www.tandfonline.com/lncn.

and replication, which are major steps of cell growth and division.[5] Thus, knowing and understanding drug-DNA interactions is important to comprehend the mode of action of any anticancer drug targeting DNA. DNA offers a number of sites for different covalent and noncovalent interactions with the drugs.

The field of anticancer metallodrugs is dominated by platinum-based compounds and the so-called "DNA paradigm", which presumes that the mechanism of action of metallodrugs relies on direct DNA damage.[6] The quest for alternative drugs to the well-known cisplatin and its derivatives, which are still used in more than 50% of the treatment regimes for patients suffering from cancer, is highly desirable.[7,8] The development of more efficient anticancer drugs with improved selectivity and diminished toxic side effects is currently an area of intense research. With the objective of developing compounds with a new mode of action in comparison to the established anticancer drugs cisplatin, carboplatin, and oxaliplatin for treatment of a broader range of tumors and with fewer side effects, many metal complexes were investigated in recent years for their tumour inhibiting properties.[9] New metal-based anticancer drugs may be able to widen the spectrum of treatable cancers, reduce toxic side effects, and overcome platinum resistance.

Ruthenium is the most attractive metal owing to its chemical and air stability, structural diversity, low toxicity and ability to mimic iron binding in biological system, which finally supported them as highly potent anticancer agents rather than platinum-based drugs.[10–12] Due to unique photophysical properties, ruthenium complexes have been widely applied in DNA probing, cellular imaging, protein monitoring, and anticancer activity.[13–20] Presently, ruthenium complex NKP-1339 (trans-[tetrachloridobis (1H–indazole) ruthenate(III)]) has successfully entered into the clinical trials.[21,22]

Changes in the structure of main ligand could be used to attain diverse DNA binding ability of ruthenium(II) complexes. Therefore, extensive studies on different structured ligands are necessary to further elucidate the DNA binding ability and its mechanism of Ru(II) complexes and discover some new potential anticancer reagents. In this article, we report the synthesis, characterization, DNA binding, light switching, photocleavage, cytotoxicity, and antimicrobial activity studies of the ligand 2-(4-(benzyloxy) phenyl)-1H-imidazo[4,5-f][1, 10]phenanthroline (BOPIP) and four of its ruthenium(II) complexes. $[Ru(phen)_2(BOPIP)]^{2+}$ **(1)**, $[Ru(bpy)_2(BOPIP)]^{2+}$ **(2)**, $[Ru(dmb)_2(BOPIP)]^{2+}$ **(3)**, $[Ru(Hdpa)_2(BOPIP)]^{2+}$ **(4)** (Scheme 1) The absorption & emission studies, viscosity measurements, and photocleavage studies show that the four complexes predominantly interact with DNA by an intercalative mode. The cytotoxicity of these compounds evaluated by 3-(4,5-dimethylthiazol-2-yl)2,5-diphenyltetrazolium bromide (MTT) assay.

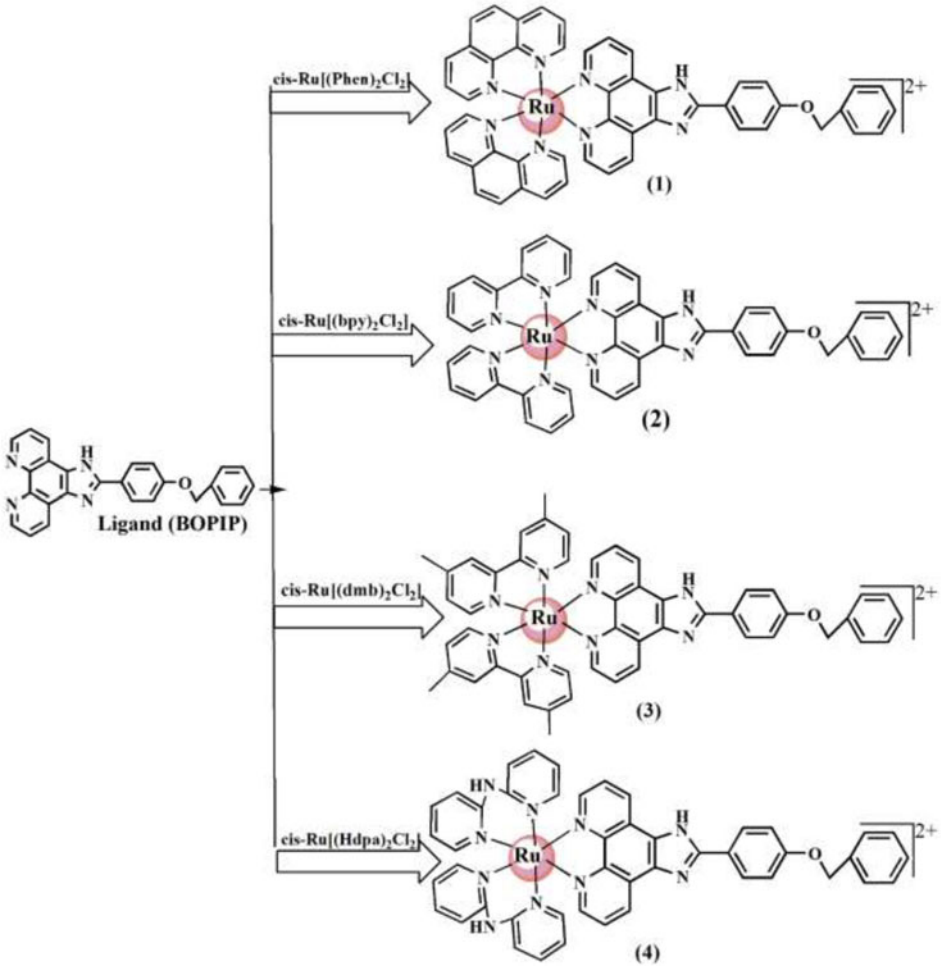

Scheme 1. Schematic synthetic route for the preparation of complexes 1, 2, 3 and 4, Where 1 = $[Ru(Phen)_2BOPIP]^{2+}$, 2 = $[Ru(bpy)_2\ BOPIP]^{2+}$, 3 = $[Ru(dmb)_2\ BOPIP]^{2+}$, 4 = $[Ru(Hdpa)_2\ BOPIP]^{2+}$.

The cytotoxicity studies show that these compounds exhibit efficient activity against HeLa (human cervical cancer cell line) cell lines in a dose-dependent manner. The antimicrobial activity experiments show that these compounds exhibit decent antimicrobial activity.

2. Materials and methods

2.1. Materials

All reagents and solvents of analytical grade were commercial products and were used as received unless otherwise stated. 1,10-Phenanthroline-5,6-dione,[23] cis-$[Ru(phen)_2Cl_2]$. $2H_2O$, cis-$[Ru(bpy)_2Cl_2].2H_2O$, cis-$[Ru(dmb)_2Cl_2].2H_2O$,[24] and cis-$[Ru(Hdpa)_2Cl_2].2H_2O$[25] were synthesized according to literature

procedures. 4-(benzyloxy) benzaldehyde, $RuCl_3.3H_2O$, and MTT were procured from Sigma-Aldrich. 1,10-Phenanthroline monohydrate, 2,2′-bipyridine (bpy), 4,4′-dimethyl-2,2′-bipyridine (dmb), and 2,2′-dipyridyl amine (Hdpa) were acquired from Merck. Calf thymus DNA (CT-DNA) was bought from Aldrich, Supercoiled pBR322 plasmid DNA (stored at −20 °C) was obtained from Fermentas Life Sciences and was used as received. Agarose was purchased from Genei. Ultrapure Milli-Q water (18.2 mX) was used in all experiments and for preparing various buffers double-distilled water was used. The HeLa human cervical carcinoma cell line was obtained from NCCS, Pune, and was maintained in RPMI 1640 standard (Sigma Aldrich) supplemented with 10% (v/v) fetal bovine serum, 2 m.mol L-glutamine, 4.5 g L-1 glucose, 19 nonessential amino acids, and 19 antibiotics consisting of penicillin/streptomycin, gentamicin, amphotericin B, and nystatin (basal growth medium). Binding of the complexes with CT-DNA was studied in tris(hydroxymethyl)aminomethane (Tris)–HCl buffer (5 m.mol Tris–HCl, 50 m.mol NaCl, pH 7.2). A solution of CT-DNA in Tris–HCl buffer gave a ratio of UV absorbance at 260 and 280 nm of 1.8:1 to 1.9:1, indicating the DNA was sufficiently free of protein.[26] The concentration of DNA per nucleotide was determined spectrophotometrically using a molar absorptivity of 6,600 M^{-1} cm^{-1} (260 nm).[27] Concentrated stock solutions of CT-DNA were prepared in buffer and were determined by the UV absorbance at 260 nm after 1:100 dilutions. Stock solutions were stored at 4 °C and used after not more than 4 days. Concentrated stock solutions of metal complexes were prepared by dissolving calculated amounts of metal complexes in DMSO and diluted suitably with the corresponding buffer to the concentrations required for all the experiments.

2.2. Physical measurements

The UV-Vis spectra was recorded on Shimadzu UV-2600 spectrophotometer. Cary Eclipse instrument serial number (MY12400004) Spectro fluorometer was used to record the luminescence spectral data for determining the binding constant values. IR spectra were recorded on a PerkinElmer 1605 Fourier transform IR spectrometer by means of KBr disks. ^{1}H and ^{13}C NMR spectra were recorded with a Bruker 400-MHz spectrometer with dimethyl-d6 sulfoxide (DMSO-d6) as the solvent and tetramethylsilane as the internal standard at room temperature. Elemental microanalysis (C, H, and N) was conducted by using PerkinElmer 240 elemental analyser. Electrospray ionization mass spectrometry (ESI–MS) mass spectra were recorded with a Quattro LC triple quadrupole mass spectrometer fortified with the MassLynx software program (Micromass, Manchester, UK).

2.3. Synthesis and characterization of ligand and complexes

The 1,10-phenanthroline-5,6-dione (Phendione),[23] cis-[Ru(phen)$_2$Cl$_2$], cis-[Ru(bpy)$_2$Cl$_2$], cis-[Ru(dmb)$_2$Cl$_2$], and cis-[Ru(Hdpa)$_2$Cl$_2$][24,25] were synthesized according to reported literature methods. Schematic diagram of Ru(II) complexes were shown in Scheme 1.

2.4. Synthesis of ligand [BOPIP]

The ligand was synthesized according to the procedure in the literature.[28] A mixture of phendione (0.53 g, 2.50 m.mol), 4-(benzyloxy) benzaldehyde (0.743 g, 3.50 m.mol), ammonium acetate (3.88 g, 50.0 m.mol) is liquified in glacial acetic acid (25 ml) and the ensuing solution was refluxed for 5h. A clear wine-red colour solution attained. The above solution was cooled to room temperature and transferred into distilled water, drop wise addition of Conc. NH_3 form a yellow precipitate, which was collected, washed with H_2O and dried. The crude product recrystallized with $C_5H_5N.H_2O$ and dried (Yield: 81.04%). Anal. Data for $C_{26}H_{18}N_4O$: Calcd(%): C, 77.59; H, 4.51; N, 13.9; found(%): C, 77.64; H, 4.45; N, 13.76. ES-MS(m/z) Calc: 402; found: 403 $[M+H]^+$. ^{1}H–NMR (DMSO-d$_6$, 400 MHz): δ 8.93(d,2H), 8.26(d, 2H), 7.88(m, 5H), 7.44(t, 2H),7.27(d, 2H), 7.1(d,2H), 5.22(s,2H). ^{13}C[^{1}H] NMR (400 MHz, DMSO-d$_6$, ppm): δ153.8, 153.1, 140.4, 137, 128.2, 122.6, 115.4, 114.8, 69.8. IR (KBr, cm^{-1}): 3641 (ν, N-H), 1118 (ν, C-N), 1240 (ν, C-O-C).

2.5. Synthesis of complexes

2.5.1. [Ru(phen)$_2$(BOPIP)](ClO$_4$)$_2$.2H$_2$O(1)

Cis-[Ru(Phen)$_2$Cl$_2$].2H$_2$O (0.284 g, 0.5 m.mol), BOPIP (0.201 g, 0.5 m.mol) dissolved in ethanol (25 ml) plus water (15ml) mixture and refluxed for 8h at 120 °C under N_2 atmosphere. When the light purple colour solution was obtained, it was cooled to room temperature and an equal volume of saturated aqueous $NaClO_4$ solution was added under vigorous stirring. The yellow precipitate was collected and washed with small amounts of water, ethanol and diethyl ether, then dried under vacuum (yield: 78%). Anal. data for $RuC_{50}H_{34}N_8O$: calcd (%): C, 69.51; H, 3.97; N, 12.97; found: C, 69.62; H, 3.88; N, 12.81. ES-MS(m/z) cal: 864; found: 866 $[M+H]^{+2}$. ^{1}H–NMR (DMSO-d$_6$, 400 MHz): δ 9.06(d,6H), 8.79(d, 6H), 8.21(d, 4H), 8.09(d, 2H),7.79(m, 6H), 7.2(d,2H), 5.25(s,2H). ^{13}C[^{1}H] NMR (400 MHz, DMSO-d$_6$, ppm): δ 160.5, 153.2, 147.7, 137.2, 132.2, 130.9, 128.9, 128.2, 126.8, 122.5, 116.0, 115.7, 69.9. IR (KBr, cm^{-1}): 3475 (ν, N-H), 1116 (ν, C-N), 1143 (ν, C-O-C), and 626 (ν, Ru-N).

2.5.2. $[Ru(bpy)_2(BOPIP)](ClO_4)_2.2H_2O(2)$

This complex was synthesized by adopting the same procedure as described above for Complex 1. taking a mixture of cis-$[Ru(bpy)_2Cl_2].2H_2O$ (0.260 g, 0.5 m.mol), BOPIP (0.201 g, 0.5 m.mol) (yield: 78%). Anal. data for $RuC_{46}H_{34}N_8O$: calcd(%): C, 67.72; H, 4.20; N, 13.73; found(%): C, 67.82; H, 4.23; N, 13.63. ES-MS(m/z) calc: 816; found: 817 $[M+H]^{+1}$. ^{1}H–NMR (DMSO-d_6, 400 MHz): δ 9.10(d,2H), 8.9(d, 4H), 8.84(d, 2H), 8.11(t, 4H),8.28(t, 4H), 7.86(d, 2H), 7.61(d,4H), 7.44(t, 2H), 7.34(m, 5H), 7.22(d,2H), 5.25(s,2H). ^{13}C[^{1}H] NMR (400 MHz, DMSO-d_6, ppm): δ 160.6, 157.2, 153.2, 151.8, 138.4, 137.1, 128.9, 128.3, 124.9, 122.5, 116.0, 115.7, 69.9. IR (KBr, cm^{-1}): 3444 (ν, N-H), 1078 (ν, C-N), 1143 (ν, C-O-C), and 626 (ν, Ru-N).

2.5.3. $[Ru(dmb)_2(BOPIP)](ClO_4)_2.2H_2O(3)$

This complex was synthesized as described above by taking a mixture of cis-$[Ru(dmb)_2Cl_2].2H_2O$ (0.288 g, 0.5 m.mol), BOPIP (0.201 g, 0.5 m.mol) (yield: 72.71%). Anal. data for $RuC_{50}H_{42}NO_9$: calc. C, 53.82; H, 4.04; Cl, 6.76; N, 12.02; O, 13.73; Ru, 9.64; found: C, 54.01; H, 4.32; Cl, 6.60; N, 11.94; O, 13.82; Ru, 9.50. ES-MS(m/z) calc: 1048; found: 1050 $[M+H]^{+2}$. ^{1}H–NMR (DMSO-d_6, 400 MHz): δ 8.75(d, 6H), 8.28(d, 2H), 8.07(s, 4H), 7.66(d, 4H), 7.44(t, 2H),7.17(m, 5H), 5.24(s,2H), 2.46(s, 12H). ^{13}C[^{1}H] NMR (400 MHz, DMSO-d_6, ppm): δ 160.5, 156.7, 150.0, 137.1, 132.2, 128.9, 128.2, 127.2, 122.6, 115.7, 69.9, 51.0. IR (KBr, cm^{-1}): 3444 (ν, N-H), 1133 (ν, C-N), 1141 (ν, C-O-C), and 624 (ν, Ru-N).

2.5.4. $[Ru(Hdpa)_2(BOPIP)](ClO_4)_2.2H_2O(4)$

This complex was synthesized as described above by taking a mixture of cis-$[Ru(Hdpa)_2Cl_2].2H_2O$ (0.19 g, 0.5 m.mol), BOPIP (0.201 g, 0.5 m.mol) (yield: 52.71%). Anal. data for $RuC_{47}H_{42}Cl_2N_9O_9$: calc. C, 53.82; H, 4.04; Cl, 6.76; N, 12.02; O, 13.73; Ru, 9.64; found: C, 54.01; H, 4.32; Cl, 6.60; N, 11.94; O, 13.82; Ru, 9.50. ES-MS(m/z) calc: 1048; found: 1050 $[M+H]^{+2}$. ^{1}H–NMR (DMSO-d_6, 400 MHz): δ 8.96(d, 4H), 8.25(d, 2H), 8.05(d, 2H), 7.74(t, 6H), 7.43(d, 2H), 6.97(m, 5H), 6.9(d, 6H), 5.24(s,2H), 4.2(s, 2H). ^{13}C[^{1}H] NMR (100 MHz, DMSO-d_6, ppm): δ 160.5, 153.8, 153.1, 137.1, 128.9, 128.2, 122.6, 115.9, 69.9. IR (KBr, cm^{-1}): 3444 (ν, N-H), 1133 (ν, C-N), 1141 (ν, C-O-C), and 624 (ν, Ru-N).

2.6. DNA-binding and photocleavage experiments

2.6.1. UV-Visible absorption spectral studies

The DNA-binding studies were conducted at room temperature. Concentrated stock solutions of metal complexes were prepared by

dissolving calculated amounts of metal complexes in DMSO and diluted accordingly with the corresponding buffer to the concentrations required for all the experiments. The absorption titrations were performed in Tris–HCl buffer. The absorption titrations of the complex in buffer were performed using a fixed complex concentration (20μl), to which increments of the DNA stock solution was added. Ru–DNA solutions were incubated for 5 min before the absorption spectra were recorded. The intrinsic binding constants K_b of these complexes with regard to DNA were calculated by using the following equation.[29]

$$[DNA]/(\varepsilon_a - \varepsilon_f) = [DNA]/(\varepsilon_b - \varepsilon_f) + 1/K_b(\varepsilon_b - \varepsilon_f) \quad (1)$$

where [DNA] is the concentration of DNA, ε_a, ε_b and ε_f correspond to the apparent absorption extinction coefficient (A_{obsd}/[complex]), the extinction coefficient for the complex in the fully bound form and the extinction coefficient for the free complex respectively. The graph was plotted between [DNA]/(ε_a-ε_f) versus [DNA] gave the intrinsic binding constant K_b. The K_b value obtained from the ratio of slope to the intercept.

2.6.2. Florescence (Luminescence) spectral studies

The luminescence titrations were performed similarly to the absorption titrations using Tris-HCl buffer. To the fixed metal concentration (10 μl), various concentrations (10–200 μl) of DNA were added. The binding constant was calculated using Scatchard equation.[30]

$$C_b = C_t\left[(F - F_0)/(F_{max} - F_0)\right] \quad (2)$$

where C_t is the total complex concentration, F is the observed fluorescence emission intensity at a given DNA concentration, F_0 is the intensity in the absence of DNA, and F_{max} is when the complex is maximum bound to DNA. From the Scatchard plot of r/C_f versus r, where r is the C_b/[DNA] and C_f is the concentration of the free complex, the negative slope gives the intrinsic binding constant K_b of the complexes based on the relation

$$r/C_f = K_b(1 - nr) \quad (3)$$

Quenching studies with $[Fe(CN)_6]^{4-}$ were extended under this luminescence experiment for further understanding the binding ability of these complexes with DNA. We also observed an interesting thing that these complexes are exhibiting the light switch on/off effect by taking the same concentrations of Co^{2+} and Na_2EDTA solutions in ideal concentrations of complex in fluorescence titrations.

2.6.3. Viscosity studies

Ostwald viscometer was used for the viscosity studies, Ostwald viscometer was immersed in thermo stated water bath maintained a constant temperature ($30 \pm 0.1\,^{\circ}C$) by using BPE buffer (6 m.mol Na_2HPO_4, 2 m.mol NaH_2PO_4, 1 m.mol Na_2EDTA, pH = 7.0). The used CT-DNA samples approximately 200 base pairs in average length were prepared by sonication to minimize the complexes arising from DNA flexibility.[31] Using the digital stopwatch, the flow time was recorded and each sample was repeated thrice. The recorded data were presented as $(\eta/\eta_0)^{1/3}$ versus concentration of [Ru(II)]/[DNA], where η is the viscosity of DNA in the presence of the complex, and η_0 is the viscosity of DNA alone. Viscosity values were calculated from the observed flow time of DNA-containing solutions (t) corrected for the flow time of the buffer alone (t_0).

2.6.4. Photocleavage experiment

For the gel electrophoresis experiments pH 8.0 buffer of 40 m.mol Tris base, 20 m.mol acetic acid, and 1 m.mol EDTA was used. A buffer of 10 m.mol Tris–HCl and 1 m.mol Na_2EDTA was used for dilution of pBR322 DNA. Supercoiled pBR322 DNA (0.1 µg/µL) was treated with ruthenium(II) complexes with concentrations of 20, 40, 80 µl, and the mixtures were irradiated at room temperature with a UV lamp (365 nm, 10 W) for 60 min. A loading buffer containing 25% bromophenol blue, 0.25% xylene cyanole, and 30% glycerol (2 µL) was added. The samples were then analysed by 0.8% agarose gel electrophoresis at 50 V for 2 h. The gel was stained with 2 µL (from 1 mg/100 µL) ethidium bromide and photographed under UV light.[32] The gels were viewed with a gel documentation system and photographed using a CCD camera (Alpha Innotech).

[**CAUTION:** *Ethidium bromide is a mutagen and potential carcinogen. Gloves should be worn and care should be taken when handling. UV light is damaging to eyes and exposed skin. Protective eyewear and apron should be worn at all times.*]

The photocleavage experiments were also performed with singlet oxygen ($^1O_2$) inhibitor Histidine and Hydroxyl free radical ($^{\cdot}OH$) inhibitor Mannitol to establish the reactive species responsible for the photoactivated cleavage of the plasmid.

2.7. Antimicrobial studies

Antimicrobial studies were performed using standard disk diffusion method.[33] The antibacterial activity of the complexes was studied against *Escherichia coli* and *Staphylococcus aureus*. Each of the ruthenium(II) complex was dissolved in DMSO at different concentrations of 10, 20, and

40 µg. Paper disks of Whatman filter paper no. 1 were sterilized in an autoclave. The paper disks saturated with 10 µL of the ruthenium(II) complex were placed aseptically in Petri dishes containing LB agar medium inoculated separately with *E. coli* and *S. aureus*. The Petri dishes were incubated at 37 °C, and the inhibition zones were recorded after 24 h of incubation. The experiments were repeated twice and the average value was taken. The results were also compared with the results for the standard antibacterial drug Ampicillin.

2.8. Molecular docking studies

Accelry's Discovery Studio (version 2.1) was used to design lead molecules, estimate the docking interactions of a complex of drug and protein binding, and number of bonds formed by ligand with the target. The molecular docking of ruthenium complexes 1, 2, 3 and 4 was performed using LibDock.[34] LibDock is a high-throughput algorithm for docking ligands into an active binding site on the receptor, which is also a site-features docking algorithm. Accelry's CHARMm force field was used throughout the simulation before running LibDock. The crystal structure of human DNA topoisomerase 1 (TOP1) receptor was downloaded from RCSB PDB (PDB ID-1T8I), after downloading the PDB format of the protein, all the water molecules of the protein were removed by using Discovery Studio and stabilizing the charges, filling the missing residues, and generating the side chains, according to the parameters available. The receptor should be in a biologically active and stable state. After the receptor is constructed, the active site within the receptor should be recognized. The receptor may have many active sites but the one of the interest should be selected. Ruthenium complexes were sketched using the tools Chemsketch and used to dock into the target binding site. Ruthenium complex conformations aligned to receptor interaction sites and the best poses were reported at the end of docking simulations. The scoring functions have been used to estimate binding affinity to screen out active and inactive compounds during the process of virtual screening.[35]

2.9. Cytotoxicity assay in vitro (MTT Assay)

Standard MTT assay was conducted as described in the literature.[36] Cells were placed in 96-well microassay culture plates (8×10^3 per well) in 200 µL and were grown overnight at 37 °C in a 5% CO_2 incubator. Complexes 1–4, in the concentration range 1–100 µM, dissolved in DMSO (Sigma-Aldrich), were added to the wells. Control wells were prepared by addition of culture medium (200 µL). Wells containing culture medium

without cells were used as a negative control and cisplatin was used as a positive control. DMSO was used as the vehicle control. A stock solution of cisplatin (10 m.mol in DMSO) was freshly prepared for every experiment. After 48 h, 20 μL of MTT solution [5 mg/mL in phosphate-buffered saline (PBS)] was added to each well and the plates were wrapped in aluminium foil and incubated for 4 h at 37 °C. The purple formazan product was dissolved by addition of 100 μL of 100% DMSO to each well. The absorbance was monitored at 620 nm using a 96-well plate reader. The stock solutions of the metal complexes were prepared in DMSO, and in all experiments, the percentage of DMSO was maintained in the range of 0.1–2%. DMSO by itself was found to be nontoxic to the cells until a concentration of 2%. Data were collected for three replicates each to obtain the mean values. The IC_{50} values were determined by plotting the percentage viability versus concentration on a logarithmic graph and reading the concentration at which 50% of cells remained viable relative to the control.

3. Results and discussion

3.1. Electronic absorption titrations

Electronic absorption spectroscopy is the common means to study the interaction between metal complexes and DNA.[37] For metallointercalators, DNA binding is associated with hypochromism and a redshift in the metal to ligand charge transfer (MLCT) and ligand bands.[38] This is primarily due to the intercalation, involving strong stacking interactions between an aromatic chromophore and the base pairs of DNA. The extent of the hypochromism in a UV–visible band is consistent with the strength of the interaction.[39] Thus, to provide evidence for the possibility of binding of each complex to CT-DNA, spectroscopic titrations of solutions of each of the complexes with several concentrations of CT-DNA were examined. A characteristic spectral curve of the complex at different DNA concentrations is shown in Figure 1. As the DNA concentration is increased, the MLCT bands of 1 at 453 nm, 2 at 462 nm, 3 at 467 nm, and 4 at 468 nm exhibit hypochromism of about 14.46, 13.74, 11.64, and 15.01%, respectively, and bathochromism of about 2–5 nm. To further elucidate the binding strength of the complexes with regard to DNA, the intrinsic binding constant K_b was determined in each case by monitoring the changes in their absorbance in the MLCT band with increasing concentration of CT-DNA. The K_b values of 1, 2, 3, and 4 are 7.1×10^4 M^{-1}, 3.4×10^4 M^{-1}, 2.5×10^4 M^{-1}, and 8.3×10^4 M^{-1}, respectively. The values are smaller than that of those DNA metallointercalators, such as $[Ru(bpy)_2(PPIP)]^{2+}$ $K_b = (4.3\ (\pm 0.40) \times 10^4\ M^{-1})$, $[Ru(phen)_2(PPIP)]^{2+}$ $K_b = (1.13\ (\pm 0.30) \times 10^5\ M^{-1})$ and

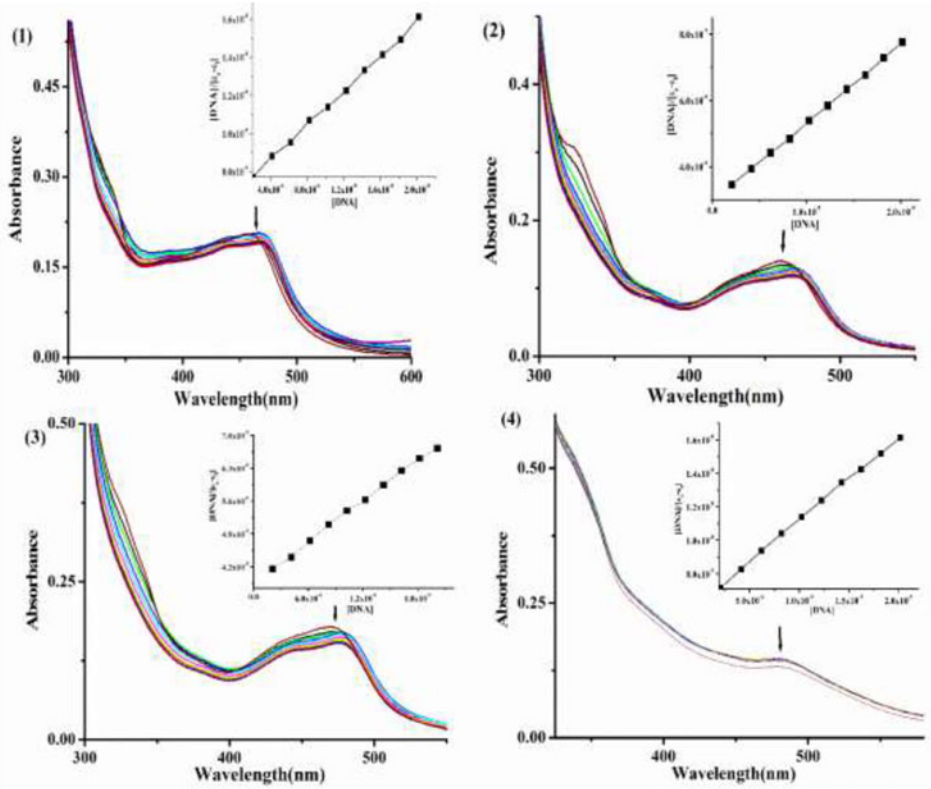

Figure 1. Absorption spectra of complexes 1–4 in absence and presence of CT-DNA in Tris-HCl buffer. Arrow shows hypochromism and bathochromism upon the increase of DNA concentration. Inserted plot,[DNA]/(ε_a-ε_f) versus [DNA] for the titration of DNA with Ru(II) complexes, which gives intrinsic binding constant (K_b).

$[Ru(bpy)_2(dppz)]^{2+}$ (dppz = dipyrido-[3,2-a:2′,3′-c]phenazine, $K_b > 10^6$ M^{-1}), but bigger than that of the parent complex $[Ru(phen)_3]^{2+}$ $K_b = (5.5 \times 10^3\ M^{-1})$.[38,40,41] Since the intercalator is common in all the four complexes, the different DNA binding properties of the four complexes are due to their diverse ancillary ligands. Going from bpy to phen, the planar area and hydrophobicity increases, which may lead to a greater binding affinity for DNA. The four additional methyl groups in complex 3 relative to complex 2 employ some steric hindrance, thus averting the complex from intercalating as effectively, and so instigating a decrease in the binding constant. The flexible nonplanar hdpa ligands approach more closely and coordinate to ruthenium(II) more strongly than the rigid phen ligands[42] and the NH group in Hdpa may employ some added interactions such as hydrogen bonding with functional groups present on the edge of the DNA.[43] This would contribute significantly to the greater binding constant in contrast to the other three complexes. The K_b values of all the complexes studied are in the order $4 > 1 > 2 > 3$.

3.2. Luminescence titrations

To further understand the exact nature of the complex binding to DNA, luminescence titration experiments were performed at a fixed metal complex concentration (5 μM) in Tris buffer (pH 7.2) at ambient temperature. The change of emission intensity is related to the extent to which the complex enters into the hydrophobic environment inside the DNA. Figure 2 shows the fluorescence excitation and emission spectra for the free and bound complexes 1–4 in the presence of different amounts of CT-DNA. Excitation wavelengths of 453, 462, 467, and 468 nm were used for fluorescence measurements of complexes 1, 2, 3, and 4, respectively and emission wavelength found to be 602, 610, 618, and 627 nm. When the CT-DNA was added to the solution of the complexes 1-4, the fluorescence intensity was found to increase. The fluorescence intensities of complexes 1, 2, 3, and 4 increased by 3.26, 3.18, 3.11, and 3.83 times, respectively, compared with the intensities in the absence of CT-DNA. The emission enhancement of the complexes 1-4 in the presence of CT-DNA is much smaller than that observed for complexes $[Ru(phen)_2(PPIP)]^{2+}$, $[Ru(bpy)_2(PPIP)]^{2+}$ and $[Ru(dmb)_2(PPIP)]^{2+}$.[41] This implies that $[Ru(phen)_2(PPIP)]^{2+}$, $[Ru(bpy)_2(PPIP)]^{2+}$ and $[Ru(dmb)_2(PPIP)]^{2+}$ may interact with CT-DNA more strongly and when the complex intercalates between the DNA base pairs, the mobility of the complex is restricted at the binding site and the hydrophobic

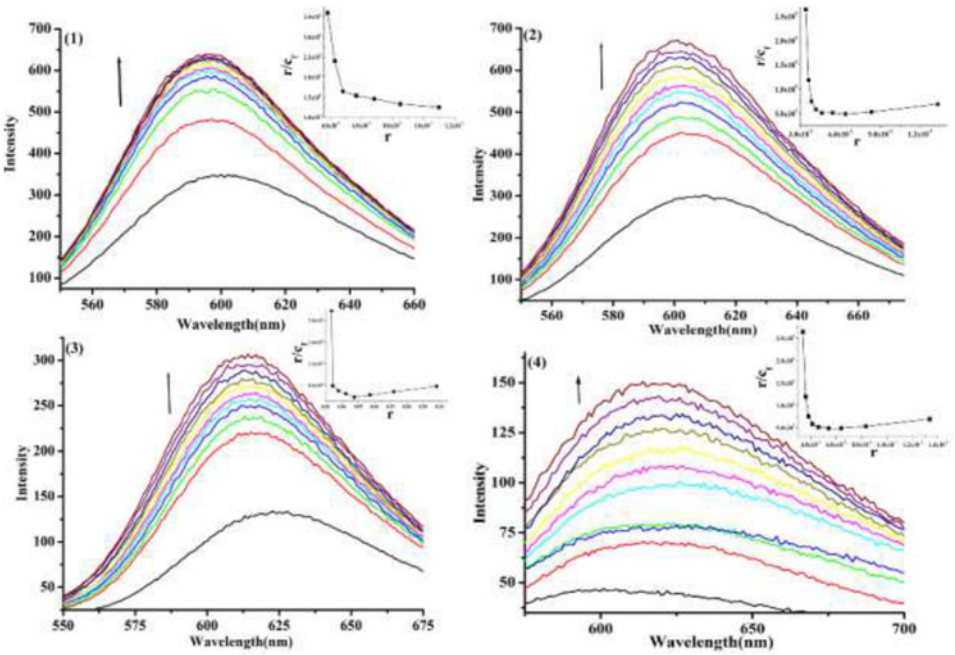

Figure 2. Emission spectra of complexes 1–4 in Tris-HCl buffer upon addition of CT-DNA. The arrow shows the intensity change upon the increase of DNA concentration. Inset: Scatchard plot of above complex, which gives binding constant (Kb).

environment inside the DNA helix reduces the accessibility of solvent water molecules to the complex, leading to a decrease of the vibrational modes of relaxation. The intrinsic binding constant from the fluorescence data was obtained from a modified Scatchard equation[30] through a plot of r/Cf versus r, where r is the binding ratio Cb/[DNA] and C_f is the free ligand concentration. Scatchard plots for the complexes were constructed from luminescence spectra, and the binding constants (K_b) were 7.29×10^4 M^{-1}, 3.61×10^4 M^{-1}, 2.57×10^4 M^{-1}, and 9.8×10^4 M^{-1} for 1, 2, 3, and 4, respectively. The binding constants calculated are in comparable with the absorption spectra.

3.2.1. Quenching studies

Steady-state emission quenching experiments using $[Fe(CN)_6]^{4-}$ as a quencher may provide further information about complexes binding to DNA, but cannot be used to determine the mode of binding. In quenching experiments, to maintain the ionic strength so that the quenching curves remain nonlinear, KCl was added along with $K_4[Fe(CN)_6]$ such that the final and total concentration was constant at 4×10^{-3} M.[44] The Stern–Volmer quenching constant (Ksv) can be determined using the Stern-Volmer equation,[45]

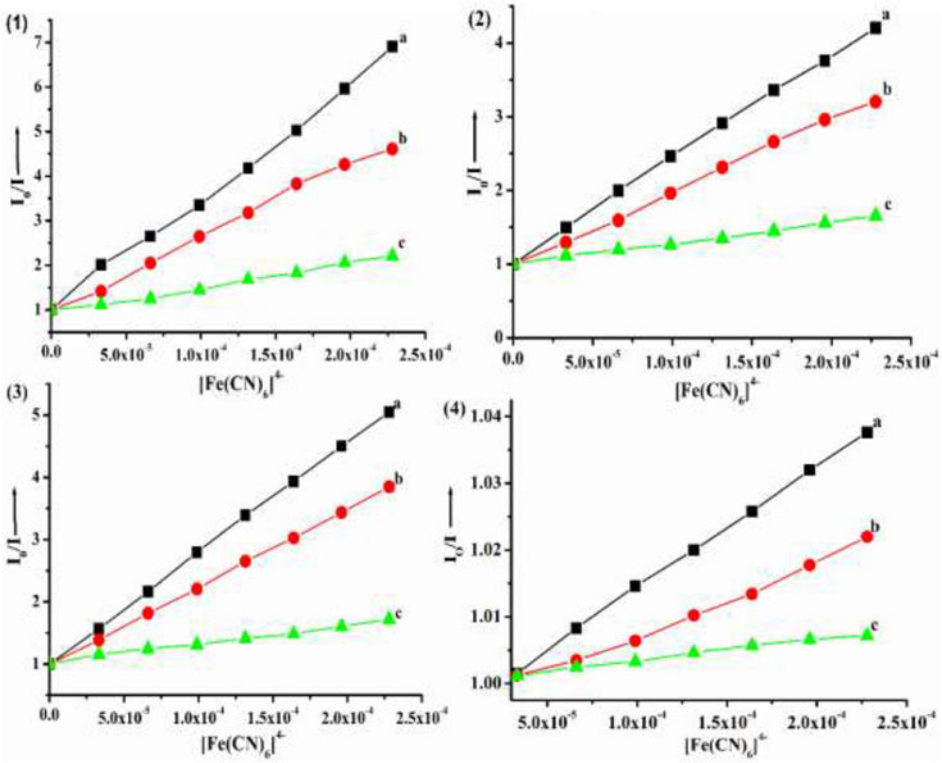

Figure 3. Quenching studies of complexes 1–4 in Tris-HCl with $[Fe(CN)6]^{4-}$ in the absence of DNA (a), presence of DNA 1:20 (b) and 1:100 (c).

Table 1. DNA binding and Ksv data for Ruthenium(II) complexes.

Complex	Absorption λ_{max} (nm) (MLCT)	Hypo chromism (%)	Absorbance binding constant (K_b)	Emission binding constant	Ksv values		
					Only Complex	Complex + DNA 1:50	Complex + DNA 1:100
$[Ru(Phen)_2BOPIP]^{+2}$ **(1)**	453	14.46	7.1×10^4	7.29×10^4	25279	16585	5542
$[Ru(bpy)_2\ BOPIP]^{+2}$ **(2)**	462	13.74	3.4×10^4	3.61×10^4	17881	12063	3053
$[Ru(dmb)_2\ BOPIP]^{+2}$ **(3)**	467	11.64	2.5×10^4	2.57×10^4	14026	9997	2804
$[Ru(Hdpa)_2BOPIP]^{+2}$ **(4)**	468	15.01	8.3×10^4	9.8×10^4	28541	17441	5847

phen: 1,10-phenanthroline, bpy: 2,2′-bipyridine, dmb: 4,4′-dimethyl-2,2′-bipyridine, bpip: 2-(4-(benzyloxy)phenyl)-1H-imidazo [4,5-f][1,10]phenanthroline, hdpa: 2,2′,-dipyridylamine, MLCT: metal-to-ligand charge transfer.

$$I_0/I = 1 + K_{SV}[Q]$$

where I_0 and I are the intensities of the fluorophore in the absence and presence of the quencher, respectively, [Q] is the concentration of the quencher, and Ksv is the linear Stern–Volmer quenching constant. In general, positively charged free complex ions may be readily quenched by $[Fe(CN)_6]^{4-}$, whereas the complex bound to DNA can be protected from the quencher as the negative charge of $[Fe(CN)_6]^{4-}$ will be repelled by the negatively charged phosphate backbone of DNA, resulting in less quenching of the bound complex compared with the free complex. Figure 3. shows the Stern–Volmer plots for the free complexes in solution and the complexes in the presence of increasing amounts of DNA. The Ksv values for all four complexes are given in Table 1. From the quenching studies it is clear that the DNA binding affinity of complexes follows the order $4 > 1 > 2 > 3$, which is consistent with other results.[38,40,46]

3.2.2. On–off–On light switching behaviour

As shown in Figure 4 the emission spectral profile of DNA bound complex **1** elucidates the switching of emission on and off when Co^{2+} and EDTA are added, respectively. The experiments were conducted using a method similar to that developed by our research group earlier.[38,46] When the complex binds to DNA (switch on), the emission intensity is high, but when we add Co^{2+} (0.03 m.mol), the emission of DNA-bound complex **1** is quenched by Co^{2+}, thus turning the light switch off,[47,48] owing to the formation of the Co^{2+}–complex **1** heterometallic complex. When EDTA (0.03 m.mol) was added to the buffer system containing Co^{2+}–complex **1**, the emission intensity recovered again (light switch on), based on the strong coordination of Co^{2+} to EDTA (EDTA– Co^{2+}) and the complex becomes free. A similar observation was made for other three complexes. The change in luminescence of the DNA-bound complex in the presence of Co^{2+} and EDTA reveals its use in the modulation of drug therapy.

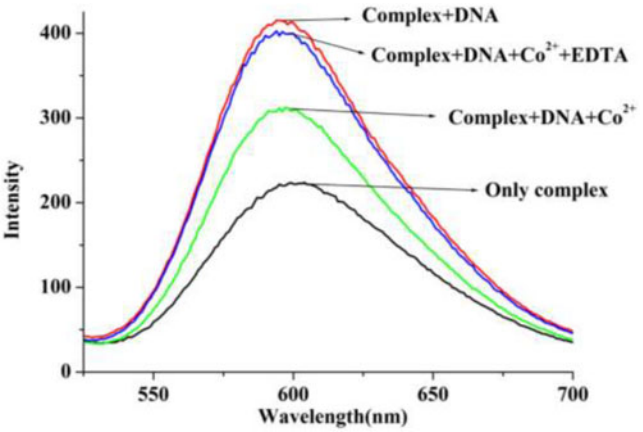

Figure 4. DNA light switch on and off experimentally showing the luminescence changes upon addition of Co^{2+}, EDTA and DNA to complex 1.

3.3. Viscosity studies

The DNA binding modes of complexes were further investigated by viscosity measurement. The viscosity measurements of DNA is regarded as the least uncertain and the critical test of a DNA binding model in solution in the absence of crystallographic data and provides strong evidence for intercalative DNA binding mode.[31,49] A classical intercalation model results in lengthening the DNA helix as base pairs are detached to accommodate the binding ligand, leading to the increase of DNA viscosity. In contrast, a partial non-classical intercalation of ligand could bend (or kink) the DNA helix and reduce its effective length.[50] For example, under suitable conditions, intercalation of dye like EtBr roots a significant increase in the overall DNA length. The effects of the complexes on the viscosity of rod-like DNA comparing with EtBr are shown in Figure 5. Though the intercalating ligand is same in all complexes, there is a small difference in the viscosity, this is due to the difference in the ancillary ligands. These further suggest that four Ru(II) complexes show an intercalative binding mode to CT-DNA, which parallel the absorption titration results. The increased degree of viscosity also supports the order of binding of the complexes to DNA as determined by other methods which follow the order EB $>4>1>2>3$ (Figure 5).

3.4. Photocleavage of pBR322 DNA

The cleavage reactions on plasmid DNA induced by ruthenium(II) complexes were performed and monitored by agarose gel electrophoresis. When circular plasmid DNA is subjected to electrophoresis, comparatively fast migration is observed for the intact supercoiled form (form I). If scission

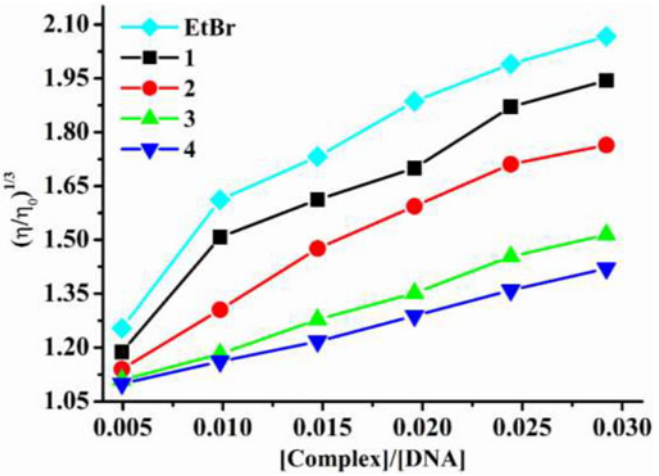

Figure 5. Viscosity studies of four complexes in BPE buffer with increasing amounts of complexes 1-4 and Ethidium bromide (EtBr) on the relative viscosity of calf thymus DNA at room temperature, a = EtBr, 1 = $[Ru(Hdpa)_2BOPIP]^{2+}$, 2 = $[Ru(Phen)_2BOPIP]^{2+}$, 3 = $[Ru(bpy)_2\ BOPIP]^{2+}$, 4 = $[Ru(dmb)_2\ BOPIP]^{2+}$.

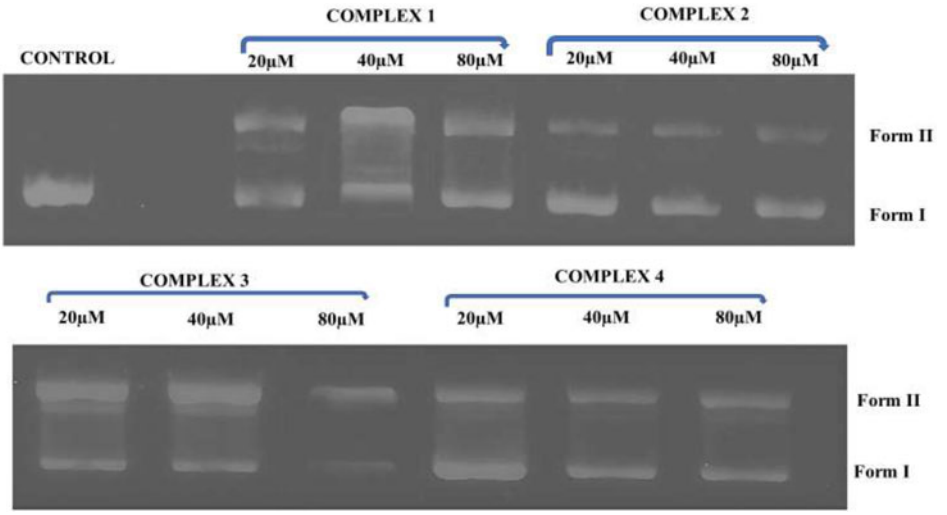

Figure 6. Photoactivated cleavage of pBR322 DNA in the absence (control) and presence of different concentrations (20, 40 and 80 μM) 0f ruthenium complexes (1–4) after irradiation under UV light for 30 minutes.

occurs on one strand (nicking), the supercoiled form will relax to generate a slower-moving open circular form (form II). If both strands are cleaved, a linear form (form III) that migrates between form I and form II will be generated.[32] Figure 6 shows gel electrophoresis separation of pBR322DNA after incubation with different concentrations of ruthenium(II) complexes and irradiation at 365 nm for 60 min. No DNA cleavage was observed for the control, in which the metal complex was absent. When the concentration of the ruthenium(II) complexes was increased, the amount of form I gradually

decreased, whereas the amount of form II increased. Under comparable experimental conditions, all complexes showed photocleavage activity. The pBR322 DNA photocleavage results for these complexes are consistent with the results obtained for other ruthenium(II) polypyridyl complexes.[51,52] To establish the reactive species responsible for the photoactivated cleavage of the plasmid, we further investigated the influence of potentially inhibitive agents. Histidine, a naturally occurring amino acid, has been widely used as a scavenger of singlet molecular oxygen ($^1O_2$) especially during biological photooxidation processes.[53] As reported $^1O_2$ reacts with histidine to form a transannular peroxide in its imidazole ring and thus loses its ability to react with other species. Histidine is also one of the most reactive biomolecules with regard to $^1O_2$ and exists in the muscle of animal tissues. In the presence of histidine (10 m.mol) (Figure 9), cleavage was absent (form II is not observed) or very much reduced compared what was observed for the complexes with DNA (absence of histidine). This indicates that $^1O_2$ plays an important role in the photocleavage mechanism. A photocleavage experiment was also conducted in the presence of mannitol, an OH radical inhibitor (Figure 7). In the presence of mannitol, form II is formed; hence, there is no change in the cleavage pattern, which indicates that the OH, radical is not responsible for cleavage and only $^1O_2$ is responsible for photocleavage of pBR322 in presence of the ruthenium(II) complexes.

3.5. Antimicrobial activity

Complexes 1–4 were screened in vitro for their microbial activity against *E. coli* and *S. aureus* at 1 mg mL-1 concentration by the standard disk

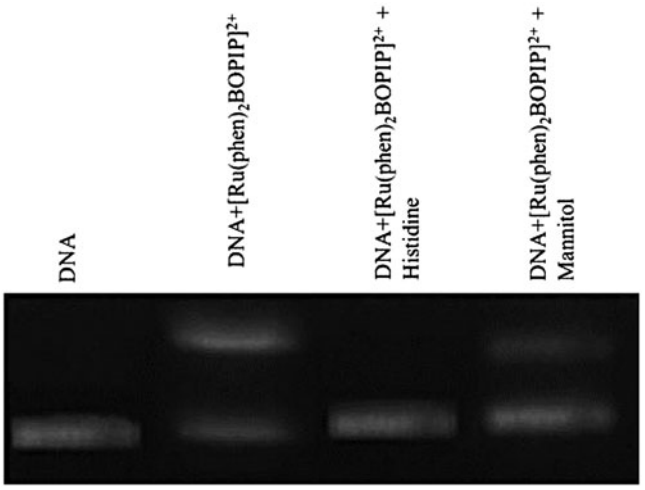

Figure 7. Photoactivated cleavage of pBR322 DNA in the presence of $[Ru(Phen)_2BOPIP]^{2+}$ complex after irradiation at 365 nm for 30 min in the presence of histidine and mannitol.

Table 2. Antibacterial activity of ruthenium(II) complexes.

	Escherichia coli (Gram negative)			*Staphylococcus aureus* (Gram positive)		
Compound	10μg	20μg	40μg	10μg	20μg	40μg
BOPIP	3			4		
$[Ru(Phen)_2BOPIP]^{+2}$ **(1)**	6.5	10.0	12	10	12	14.0
$[Ru(bpy)_2\ BOPIP]^{+2}$ **(2)**	6.0	8.0	10	9	11	12.2
$[Ru(dmb)_2\ BOPIP]^{+2}$ **(3)**	5.5	9.2	11.5	8	11.7	13.5
$[Ru(Hdpa)_2BOPIP]^{+2}$ **(4)**	5.0	8.7	10.4	7	11.2	12.5
Ampicillin			18.0			21

Inhibition zone diameter in millimetres.

method. The results are expressed as inhibition zone diameter (in millimetres) versus the control (DMSO). The DMSO control showed negligible activity as compared with the metal complexes. The antimicrobial activity increased as the concentration of the compounds increased. The antibacterial activity data for the complexes at various concentrations (Table 2) indicate that the complexes exhibited appreciable activity against *E. coli* and *S. aureus*. The activity increased with the increase in the concentrations of the complexes. The complexes were more effective against *E. coli* than against *S. aureus* but were less effective than the standard drug ampicillin. As an increase in the lipophilic character of the complex favors its permeation through the lipid layer of the bacterial membrane, it shows more activity. These results are consistent with results from earlier studies.[54,55]

3.6. Molecular docking studies

Molecular docking studies The LibDock module from Discovery Studio was used to perform the molecular docking of ruthenium complexes 1, 2, 3 and 4 with the active site pocket residues of human DNA TOP1. Human DNA TOP1 is an essential enzyme that relaxes DNA supercoiling during replication and transcription. The topoisomerase enzymes have been researched as targets for the generation of new cancer treatments because when they are inhibited in a cell, cell death results. Therefore, inhibitors of the topoisomerase enzymes have the ability to kill all cells undergoing DNA replication, reading of the DNA for protein production, or experiencing repair of DNA damage. Subsequently, cancer cells divide much more rapidly than normal cells, the cancer cells will be slaughtered by the topoisomerase inhibitors, however, some normal cells with topoisomerase activity will also be killed. DNA TOP1 is overexpressed in tumor cells and is an important target in cancer chemotherapy. All the ruthenium complexes were docked into the active site pocket of DNA TOP1, using LibDock. According to the results obtained from LibDock simulation, all ruthenium complexes were ranked by the LibDock scores. From the results, complex 4 exhibited the highest docking scores of 137.942 kcal/mol (Figure 8). The interactions and Dock scores of the

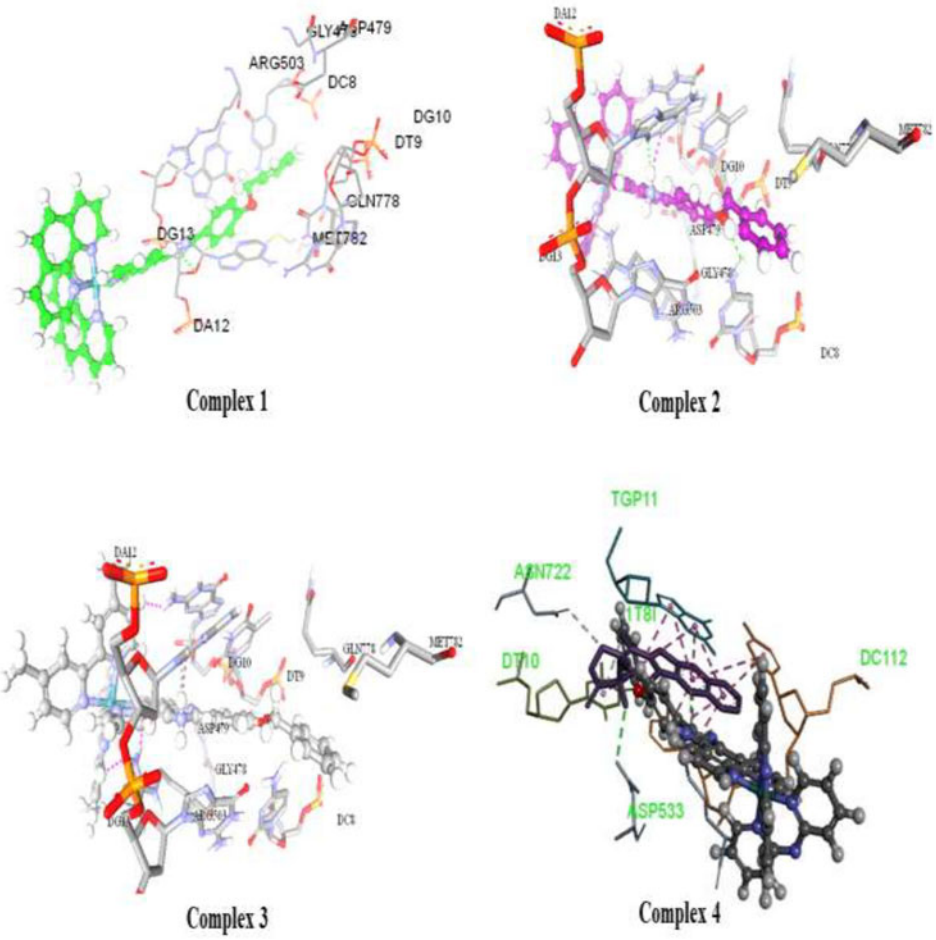

Figure 8. Molecular docking models illustrating the interaction between complexes with active site pocket residues of human DNA topoisomerase 1 (PDB ID: 1T8I) target and showing intermolecular hydrogen bonds.

Table 3. The LibDock scores and docking interactions of the ruthenium complexes (1–4) with human DNA TOP 1.

Complex	Libdock Score (K.Cal/Mole)	Interacting Residues	Interacting atoms	H-Distance
1	121.159	DC8,DT9,DG10, Gly478, Asp479, Met782, Arg503, Gln778	5:H67 - F:DA12:O4′ complex	2.2600
2	115.942	DC8, DT9, DG10, Gly478, Asp479, Met782, Arg503, Gln778	complex:H63 - F:DA12:N3 complex:H63 - F:DA12:C2 DC8:H42 - O49 complex	1.764 2.205 2.392
3	116.893	DC8, DT9, DG10, Gly478, Asp479, Met782, Arg503, Gln778	complex:H68 - F:DA12:N3 complex:H62 - F:DA12:C1′ complex:H62 - F:DA12:C2′ complex:C7 - A:ARG503:HH11	1.967 2.154 1.9070 2.0590
4	137.942	DT10, DC112, DA113, TGP11, Asn722, Asp533,	B:DT10:H3 – complex: O49	2.061

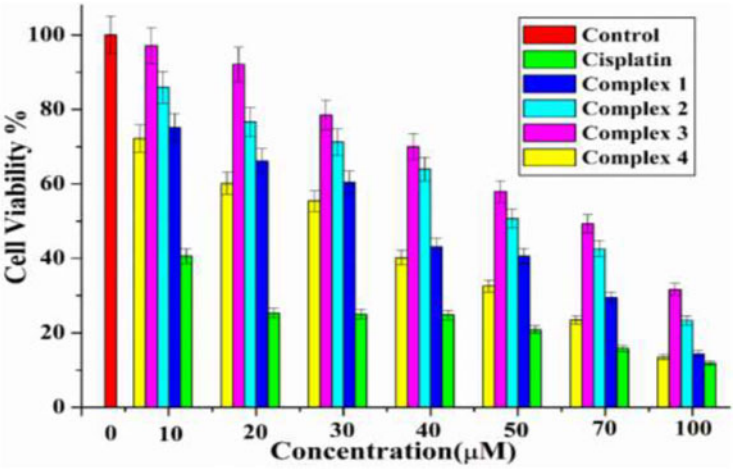

Figure 9. Cell viability of HeLa cell lines invitro treatment with complexes 1, 2, 3 and 4. Each data point is the mean standard error obtained from at least three independent experiment.

Table 4. The IC50 values for complexes 1–4 against HeLa cell lines.

S.No.	Compound	IC_{50} (μM)
1	$[Ru(Phen)_2BOPIP]^{+2}$ **(1)**	27.76
2	$[Ru(bpy)_2\ BOPIP]^{+2}$ **(2)**	31.59
3	$[Ru(dmb)_2\ BOPIP]^{+2}$ **(3)**	36.42
4	$[Ru(Hdpa)_2BOPIP]^{+2}$**(4)**	24.38
5	Cisplatin	4.81

ruthenium complexes with the active site pocket residues of human DNA TOP1 were tabulated in Table 3. The active site pocket residues of human DNA TOP1 were involved in hydrogen bonding formation with ruthenium complexes. A higher score indicates a stronger receptor–ligand-binding affinity.

3.7. In vitro cytotoxicity

The cytotoxicity activity of all four complexes and the corresponding ligand against the HeLa (human cervical cancer cell line) cell lines was evaluated by MTT assay. Cisplatin was used as a positive control and DMSO as negative control. The IC_{50} values obtained for four complexes are shown in Table 4. The tumor cells in the presence of complexes 1–4 were incubated for 48 h. The IC_{50} values for all the complexes ranged from 1 to 100 μM, suggesting that the ligand and the complexes exhibited antitumor activity against HeLa cell lines to different degrees. These compounds all exhibit relatively lower in vitro cytotoxicity against the selected HeLa cell line than cisplatin. Figure 9 showed that the cell viability decreased with increasing concentrations of complexes 1, 2, 3 and 4. Among all these, complex 4 exhibited higher in vitro cytotoxicity, with IC_{50} values of 24.38. This is may be due to the presence of an amine group (–NH–) between two pyridine moieties in Hdpa.[25]

The cytotoxicity activity of the complexes is consistent with their DNA binding abilities i.e. $4 > 1 > 2 > 3$. The obtained IC_{50} values are also comparable with the reported ruthenium (II) polypyridyl complexes.[56]

Conclusion

Four Ru(II) complexes $[Ru(phen)_2\ BOPIP]^{2+}$**(1)**, $[Ru(bpy)_2\ BOPIP]^{2+}$**(2)** $[Ru(dmb)_2\ BOPIP]^{2+}$**(3)**, $[Ru(Hdpa)_2\ BOPIP]^{2+}$**(4)** were synthesized and characterized. The absorption spectral studies, Luminescence titrations, and viscosity measurements suggest that all the four complexes bind to CT-DNA through intercalation. The intrinsic binding constants calculated through absorption studies and fluorescence spectral studies are good in agreement and complex 4 exhibits slightly higher intrinsic binding constant among four complexes. Upon irradiation, under UV light all the four complexes can cleave pBR322 DNA and proved that singlet oxygen($^1O_2$) is responsible for the cleavage of pBR322 DNA. All the four complexes exhibit the Antimicrobial activity and showed cytotoxicity against A549 (human lung tumor cell line), Du145 (human prostate cancer cell line), and HeLa (human cervical cancer cell line) cell lines. These complexes exhibit relatively lower in vitro cytotoxicity against the selected cell lines than cisplatin. Molecular docking studies support the Hydrogen bonding and Vander Wall's interactions play a major role in binding to DNA.

Acknowledgments

The University Grants Commission, New Delhi, India, is gratefully acknowledged for the support in the form of Teacher Fellowship under Faculty Development programme to one of the authors. We also extend our sincere thanks to CFRD Osmania University for providing instrumentation facilities.

References

[1] Wu, J.; Wu, S.; Shi, L.; Zhang, S.; Ren, J.; Yao, S.; Yun, D.; Huang, L.; Wang, J.; Li, W.; et al. Design, Synthesis, and Evaluation of Asymmetric EF24 Analogues as Potential Anti-cancer Agents for Lung Cancer. *Eur. J. Med. Chem.* **2017**, *125*, 1321–1331. DOI: 10.1016/j.ejmech.2016.10.027.

[2] Komor, A. C.; Barton, J. K. The Path for Metal Complexes to a DNA Target. *Chem. Commun. (Camb.)* **2013**, *49*, 3617–3630.

[3] Lin, R.; Johnson, S. G.; Connolly, P. J.; Wetter, S. K.; Binnun, E.; Hughes, T. V.; Murray, W. V.; Pandey, N. B.; Moreno-Mazza, S. J.; Adams, M.; et al. Synthesis and Evaluation of 2,7-diamino-thiazolo[4,5-*d*] Pyrimidine Analogues as Anti-tumor Epidermal Growth Factor Receptor (EGFR) tyrosine Kinase Inhibitors. *Bioorg. Med. Chem. Lett.* **2009**, *19*, 2333–2337. DOI: 10.1016/j.bmcl.2009.02.067.

[4] Zheng, Y.; Zhu, L.; Fan, L.; Zhao, W.; Wang, J.; Hao, X.; Zhu, Y.; Hu, X.; Yuan, Y.; Shao, J.; Wang, W. Synthesis, SAR and Pharmacological Characterization of Novel

Anthraquinone Cation Compounds as Potential Anticancer Agents. *Eur. J. Med. Chem.* **2017**, *125*, 902–913. DOI: 10.1016/j.ejmech.2016.10.012.

[5] Syam, S.; Abdelwahab, S. I.; Al-Mamary, M. A.; Mohan, S. Synthesis of Chalcones with Anticancer Activities. *Molecules* **2012**, *17*, 6179–6195.

[6] Hartley, J. A.; Hochhauser, D. Small Molecule Drugs - Optimizing DNA Damaging Agent-Based Therapeutics. *Curr. Opin. Pharmacol.* **2012**, *12*, 398–402.

[7] Lippert, B. *Cisplatin Chemistry and Biochemistry of a Leading Anticancer Drug Wiley*; Weinheim: Germany, **1999**.

[8] Jakupec, M. A.; Galanski, M.; Arion, V. B.; Hartinger, C. G.; Keppler, B. K. Antitumour Metal Compounds: More than Theme and Variations. *Dalton Trans* **2008**, *2*, 183–194. DOI: 10.1039/B712656P.

[9] Dyson, P. J.; Sava, G. Metal-Based Antitumour Drugs in the Post Genomic Era. *Dalton Trans.* **2006**, *16*, 1929–1933. DOI: 10.1039/b601840h.

[10] Mendoza-Ferri, M. G.; Hartinger, C. G.; Mendoza, M. A.; Groessl, M.; Egger, A. E.; Eichinger, R. E.; Mangrum, J. B.; Farrell, N. P.; Maruszak, M.; Bednarski, P. J.; et al. Transfering the Concept of Multinuclearity to Ruthenium Complexes for Improvement of Anticancer Activity. *J. Med. Chem.* **2009**, *52*, 916–925. DOI: 10.1021/jm8013234.

[11] Hartinger, C. G.; Metzler-Nolte, N.; Dyson, P. J. Challenges and Opportunities in the Development of Organometallic Anticancer Drugs. *Organometallics* **2012**, *31*, 5677–5685. DOI: 10.1021/om300373t.

[12] Gasser, G.; Ott, I.; Metzler-Nolte, N. Organometallic Anticancer Compounds. *J. Med. Chem.* **2011**, *54*, 3–25.

[13] Gill, M. R.; Garcia-Lara, J.; Foster, S. J.; Smythe, C.; Battaglia, G.; Thomas, J. A. A Ruthenium(II) polypyridyl Complex for Direct Imaging of DNA Structure in Living Cells. *Nat. Chem.* **2009**, *1*, 662–667.

[14] Vyas, N. A.; Ramteke, S. N.; Kumbhar, A. S.; Kulkarni, P. P.; Jani, V.; Sonawane, U. B.; Joshi, R. R.; Joshi, B.; Erxleben, A. Ruthenium(II) polypyridyl Complexes with Hydrophobic Ancillary Ligand as Aβ Aggregation Inhibitors. *Eur. J. Med. Chem.* **2016**, *121*, 793–802. DOI: 10.1016/j.ejmech.2016.06.038.

[15] Puckett, C. A.; Ernst, R. J.; Barton, J. K. Exploring the Cellular Accumulation of Metal Complexes. *Dalton Trans.* **2010**, *39*, 1159–1170.

[16] Cook, N. P.; Torres, V.; Jain, D.; Martí, A. A. Sensing Amyloid-β Aggregation Using Luminescent Dipyridophenazine Ruthenium(II) Complexes. *J. Am. Chem. Soc.* **2011**, *133*, 11121–11123. DOI: 10.1021/ja204656r.

[17] Chen, Y.; Qin, M. Y.; Wu, J. H.; Wang, L.; Chao, H.; Ji, L. N.; Xu, A. L. Synthesis, Characterization, and Anticancer Activity of Ruthenium(II)-β-Carboline complex*Eur. Eur. J. Med. Chem.* **2013**, *70*, 120–129.

[18] Liu, P.; Jia, J.; Zhao, Y.; Wang, K. Z. Recent Advances on Dark and Light-Activated Cytotoxity of Imidazole-Containing Ruthenium Complexes. *Mini Rev. Med. Chem.* **2016**, *16*, 272–289.

[19] Poynton, F. E.; Bright, S. A.; Blasco, S.; Williams, D. C.; Kelly, J. M.; Gunnlaugsson, T. The Development of Ruthenium(ii) Polypyridyl Complexes and Conjugates for in vitro Cellular and in vivo Applications. *Chem. Soc. Rev.* **2017**, *46*, 7706.

[20] Vuradi, R. K.; Dandu, K.; Kumar, Y. P.; Vinoda Rani, M.; Rajender Reddy, M.; Chintakuntla, N.; Ravi, C.; Thakur, S. S.; Rao, C. M.; Satyanarayana, S. Studies on the DNA Binding and Anticancer Activity of Ru(II) polypyridyl Complexes by Using a (2-(4-(Diethoxymethyl)-^{1}H-imidazo[4,5-*f*][1,10] phenanthroline)) Intercalative Ligand. *New J. Chem.* **2018**, *42*, 846. DOI: 10.1039/C7NJ03819D.

[21] Muhammad, N.; Guo, Z. Metal-based Anticancer Chemotherapeutic Agents. *Curr. Opin. Chem. Biol.* **2014**, *19*, 144–153. DOI: 10.1016/j.cbpa.2014.02.003.

[22] Sava, G.; Bergamo, A.; Bonetti, A.; Leone, R.; Muggia, F.M.; Howell, S.B. (Eds.). *Synthesis and in Vitro (Anticancer) Evaluation of η 6 -Arene Ruthenium Complexes Bearing Stannyl Ligands*; Humana Press: Totowa, **2009**,57–66.

[23] Yamada, M.; Nakamura, Y.; Hasegawa, T.; Itoh, A.; Kuroda, S.; Shimao, I. Synthesis and Properties of Diamino-Substituted Dipyrido [3,2-*a*: 2′,3′-*c*]Phenazine. *Bull. Chem. Soc. Japan* **1992**, *65*, 2007–2009.

[24] Sullivan, B. P.; Sullivan, D. J.; Salmon, B. P.; Mayer, T. J. Mixed Phosphine 2,2'-Bipyridine Complexes of Ruthenium. *Inorg. Chem.* **1978**, *17*, 3334–3341. DOI: 10.1021/ic50190a006.

[25] Rajendran, V.; Murali, M.; Suresh, E.; Sinha, S.; Somasundaram, K.; Palaniandavar, M. Mixed Ligand Ruthenium (II) Complexes of bis(pyrid-2-yl)-/bis(benzimidazol-2-yl)-Dithioether and Diimines: Study of Non-covalent DNA Binding and Cytotoxicity. *Dalton Trans.* **2008**, *7*(1),148–163. DOI: 10.1039/B710578A.

[26] Marmur, J. A Procedure for the Isolation of Deoxyribonucleic Acid from Micro-Organisms. *J. Mol. Bio.* **1961**, *3*, 208–218. DOI: 10.1016/S0022-2836(61)80047-8.

[27] Reichmann, M. E.; Rice, S. A.; Thomas, C. A.; Doty, P. A Further Examination of the Molecular Weight and Size of Desoxypentose Nucleic Acid. *J. Am. Chem. Soc.* **1954**, *76*, 3047–3053. DOI: 10.1021/ja01640a067.

[28] Steck, E. A.; Day, A. R. Reactions of Phenanthraquinone and Retenequinone with Aldehydes and Ammonium Acetate in Acetic Acid Solution. *J. Am. Chem. Soc.* **1943**, *65*, 452–456.

[29] Wolfe, A.; Shimer, G. H.; Meehan, T. Polycyclic Aromatic Hydrocarbons Physically Intercalate into Duplex Regions of Denatured DNA. *Biochemistry* **1987**, *26*, 6392–6396. DOI: 10.1021/bi00394a013.

[30] Mc Ghee, J. D.; Von Hippel, P. H. Theoretical Aspects of DNA-protein Interactions: co-operative and Non-co-operative Binding of Large Ligands to a One-dimensional Homogeneous Lattice. *J. Mol. Biol.* **1974**, *86*, 469–489. DOI: 10.1016/0022-2836(74)90031-X.

[31] Chaires, J. B.; Dattagupta, N.; Crothers, D. M. Selfassociation of Daunomycin. *Biochemistry* **1982**, *21*, 3927–3932. DOI: 10.1021/bi00260a004.

[32] Barton, J. K.; Raphael, A. L. Photoactivated Stereospecific Cleavage of Double-helical DNA by Cobalt(III) Complexes. *J. Am. Chem. Soc.* **1984**, *106*, 2466–2468. DOI: 10.1021/ja00320a058.

[33] Drew, W. L.; Barry, A. L.; Toole, R. O.; Sherris, J. C. Reliability of the Kirby-Bauer Disc Diffusion Method for Detecting Methicillin-Resistant Strains of *Staphylococcus aureus*. *Appl. Microbiol.* **1972**, *24*, 240–247.

[34] Diller, D. J.; Merz , K. M. Jr. High Throughput Docking for Library Design and Library Prioritization. *Proteins* **2001**, *43*, 113–124.

[35] Jones, G.; Willet, P.; Glen, R. C. Molecular Recognition of Receptor Sites Using a Genetic Algorithm with a Description of Desolvation. *J. Mol. Biol.* **1995**, *245*, 43–53. DOI: 10.1016/S0022-2836(95)80037-9.

[36] Mosmann, T. Rapid Colorimetric Assay for Cellular Growth and Survival: Application to Proliferation and Cytotoxicity Assays. *J. Immunol. Methods* **1983**, *65*, 45–55. DOI: 10.1016/0022-1759(83)90303-4.

[37] Barton, J. K.; Danishefsky, A.; Goldberg, J. Tris(phenanthroline)ruthenium(II): Stereoselectivity in Binding to DNA. *J. Am. Chem. Soc.* **1984**, *106*, 2172–2176. DOI: 10.1021/ja00319a043.

[38] Pyle, A. M.; Rehmann, J. P.; Meshoyrer, R.; Kumar, C. V.; Turro, N. J.; Barton, J. K. Mixed-ligand Complexes of Ruthenium(II): Factors Governing Binding to DNA. *J. Am. Chem. Soc.* **1989**, *111*, 3051–3058. DOI: 10.1021/ja00190a046.

[39] Moucheron, C.; Mesmaeker, A. K. D.; Choua, S. Photophysics of $Ru(phen)_2(PHEHAT)^{2+}$: A Novel "Light Switch" for DNA and Photo-oxidant for Mononucleotides. *Inorg. Chem.* **1997**, *36*, 584–592. DOI: 10.1021/ic9609315.

[40] Deepika, N.; Praveen Kumar, Y.; Shobha Devi, Ch.; Venkat Reddy, P.; Srishailam, A.; Satyanarayana, S. Synthesis, characterization, and DNA binding, photocleavage, cytotoxicity, cellular uptake, apoptosis, and on-off light switching studies of Ru(II) mixed-ligand complexes containing 7-fluorodipyrido[3,2-a:2′,3′c]phenazine. *J Biol Inorg Chem*, **2013**, 18, 751–766.

[41] Tan, L.-F.; Chao, H.; Li, H.; Liu, Y.-J.; Sun, B.; Wei, W.; Ji, L.-N. Synthesis, Characterization, DNA-Binding and Photocleavage Studies of $[Ru(bpy)2(PPIP)]^{2+}$ and $[Ru(phen)2(PPIP)]^{2+}$. *J. Inorg. Biochem.* **2005**, *99*, 513–528. DOI: 10.1016/j.jinorgbio.2004.10.028.

[42] Ravi Kumar, V.; Nagababu, P.; Srinivas, G.; Reddy, M. R.; Rani, M. V.; Ravi, M.; Satyanarayana, S. Investigation of DNA/BSA Binding of Three Ru(II) complexes by Various Spectroscopic Methods, molecular Docking and Their Antimicrobial Activity. *J. Coord. Chem.* **2017**, *70*, 3790–3809. DOI: 10.1080/00958972.2017.1407410.

[43] Tu, L. C.; Chen, C. S.; Hsiao, I. C.; Chern, J. W.; Lin, C. H.; Shen, Y. C.; Yeh, S. F. Synthesis of 1-Substituted Carbazolyl-1,2,3,4-tetrahydro- and Carbazolyl-3,4-dihydro-β-carboline Analogs as Potential Antitumor Agents. *Chem. Biol.* **2005**, *12*, 1317–1324.

[44] Ang, W. H.; Dyson, P. J. Classical and Non-Classical Ruthenium-Based Anticancer Drugs: Towards Targeted Chemotherapy. *Eur. J. Inorg. Chem.* **2006**, 4003–4018. DOI: 10.1002/ejic.200600723.

[45] Satyanarayana, S.; Dabrowiak, J. C.; Chaires, J. B. Tris(phenanthroline)ruthenium(II) enantiomer Interactions with DNA: mode and Specificity of Binding. *Biochemistry* **1993**, *32*, 2573–2584. DOI: 10.1021/bi00061a015.

[46] Lakowicz, J. R.; Weber, G. Quenching of Fluorescence by Oxygen. Probe for Structural Fluctuations in Macromolecules. *Biochemistry* **1973**, *12*, 4161–4170. DOI: 10.1021/bi00745a020.

[47] Shobhadevi, C.; Satyanarayana, S. Review: Synthesis, characterization, and DNA-binding Properties of Ru(II) molecular "light Switch" Complexes. *J. Coord. Chem.* **2012**, *65*, 474–486. DOI: 10.1080/00958972.2011.649736.

[48] Liu, X. W.; Shen, Y. M.; Lu, J. L.; Chen, Y. D.; Li, L.; Zhang, D. S. Synthesis, DNA-binding and Photocleavage of "light Switch" complexes $[Ru(bpy)_2(pyip)]^{2+}$and $[Ru(phen)_2(pyip)]^{2+}$. *Spectrochim. Acta. Part A*. **2010**, *77*, 522–527.

[49] Chen, M.; Li, H.; Li, Q.; Xu, Z. Luminescence Properties of [Ru(bpy)(2) MDHIP](2+) modulated by the introduction of DNA, copper(II) ion and EDTA. *Spectrochim. Acta A Mol. Biomol. Spectrosc.* **2010**, *75*, 1566–1570.

[50] Satyanarayana, S.; Dabrowiak, J. C.; Chaires, J. B. Neither DELTA.- nor.LAMBDA.-Tris(phenanthroline)Ruthenium(II) Binds to DNA by Classical Intercalation. *Biochemistry* **1992**, *31*, 9319–9324. DOI: 10.1021/bi00154a001.

[51] Satyanarayana, S.; Suh, D.; Fokt, I.; Przewloka, T.; Priebe, W.; Chaires, J. B. Parsing the Free Energy of Anthracycline Antibiotic Binding to DNA. *Biochemistry* **1996**, *35*, 2047–2053.

[52] Liu, Y. J.; Zeng, C. H.; Huang, H. L.; He, L. X.; Wu, F. H. Synthesis, DNA-binding, photocleavage, cytotoxicity and Antioxidant Activity of Ruthenium (II) polypyridyl Complexes. *Eur. J. Med. Chem.* **2010**, *45*, 564–571.

[53] Huang, H. L.; Li, Z. Z.; Liang, Z. H.; Liu, Y. J. Cell Cycle Arrest, Cytotoxicity, Apoptosis, DNA-Binding, Photocleavage, and Antioxidant Activity of Octahedral Ruthenium(II) Complexes. *Eur. J. Inorg. Chem*. **2011**, *2011*, 5538–5547. DOI: 10.1002/ejic.201100848.

[54] Tan, L. F.; Liang, X. L.; Liu, X. H. Synthesis, double Stranded DNA-binding and Photocleavage Studies of a Functionalized Ruthenium(II) complex with 7,7′-methylenedioxyphenyldipyrido[3,2-a:2′,3′-c]-Phenazine. *J. Inorg. Biochem*. **2009**, *103*, 441–447.

[55] Islam, M. S.; Hossain, M. B.; Reza, M. Y. Synthesis, Characterization and Antibacterial Activity of Mixed Ligand Complexes of Pd(II) Ions with Oxalic Acid and Heterocyclic Amines. *J. Med. Sci*. **2003**, *3*, 289–293.

[56] Morad, F. M.; Ajaily, M. M. E. L.; Gweirif, S. B. Preparation, Physical Characterization and Antibacterial Activity of Ni (II) Schiff Base Complex. *J. Sci. Appl*. **2007**, *1*, 72–78.

[57] Venkat Reddy, P.; Nagamani, C.; Reddy M, R.; Srishailam, A.; Nagasuryaprasad, K.; Deepika, N.; Yashvanth, V. V. N.; Prakasham, R. S.; Satyanrayana, S. S.; Satyanarayana, S. Synthesis and Evaluation of Invitro DNA/Protein Binding Affinity, Antimicrobial, Antioxidant and Antitumor Activity of Mononuclear Ru (II) Moxed Polypyridyl Complexes. *J. Fluoresc*. **2016**, *26*, 225–240. DOI: 10.1007/s10895-015-1705-z.